IFIC/16-66
FERMILAB-PUB-16-370-A

Prepared for submission to JCAP

Toward (Finally!) Ruling Out Z and Higgs Mediated Dark Matter Models

Miguel Escudero,[a,b] **Asher Berlin,**[c] **Dan Hooper**[b,d,e] **and Meng-Xiang Lin**[d]

[a]Instituto de Física Corpuscular (IFIC), CSIC-Universitat de València, Apartado de Correos 22085, E-46071 Valencia, Spain
[b]Fermi National Accelerator Laboratory, Center for Particle Astrophysics, Batavia, IL 60510
[c]University of Chicago, Department of Physics, Chicago, IL 60637
[d]University of Chicago, Department of Astronomy and Astrophysics, Chicago, IL 60637
[e]University of Chicago, Kavli Institute for Cosmological Physics, Chicago, IL 60637

E-mail: miguel.escudero@ific.uv.es, berlin@uchicago.edu, dhooper@fnal.gov, mxlin@uchicago.edu

arXiv:1609.09079v1 [hep-ph] 28 Sep 2016

Abstract. In recent years, direct detection, indirect detection, and collider experiments have placed increasingly stringent constraints on particle dark matter, exploring much of the parameter space associated with the WIMP paradigm. In this paper, we focus on the subset of WIMP models in which the dark matter annihilates in the early universe through couplings to either the Standard Model Z or the Standard Model Higgs boson. Considering fermionic, scalar, and vector dark matter candidates within a model-independent context, we find that the overwhelming majority of these dark matter candidates are already ruled out by existing experiments. In the case of Z mediated dark matter, the only scenario that is not already experimentally excluded is that of a fermionic dark matter candidate with an axial coupling and with a mass within a few GeV of the Z resonance ($m_{\rm DM} \simeq m_Z/2$). Several Higgs mediated scenarios are currently viable if the mass of the dark matter is near the Higgs pole ($m_{\rm DM} \simeq m_H/2$). Otherwise, the only scenarios that are not excluded are those in which the dark matter is a scalar (vector) heavier than 400 GeV (1160 GeV) with a Higgs portal coupling, or a fermion with a pseudoscalar (CP violating) coupling to the Standard Model Higgs boson. With the exception of dark matter with a purely pseudoscalar coupling to the Higgs, it is anticipated that planned direct detection experiments will probe the entire range of models considered in this study.

[1]ORCID: http://orcid.org/0000-0002-4487-8742
[2]ORCID: http://orcid.org/0000-0002-1156-1482
[3]ORCID: http://orcid.org/0000-0001-8837-4127
[4]ORCID: http://orcid.org/0000-0003-2908-4597

Contents

1 Introduction **1**

2 Z Mediated Dark Matter **2**
2.1 Fermionic dark matter 2
2.2 Scalar dark matter 5
2.3 Vector dark matter 5

3 Higgs Mediated Dark Matter **7**
3.1 Fermionic dark matter 7
3.2 Scalar dark matter 10
3.3 Vector dark matter 10

4 Caveats **14**

5 Summary and Conclusions **14**

1 Introduction

Over the past few decades, the WIMP paradigm has dominated the theoretical and experimental landscape of dark matter. Interest in dark matter in the form of weakly interacting massive particles (WIMPs) has been motivated in large part by the realization that a generic stable particle with an electroweak scale mass and interactions will freeze-out in the early universe with a thermal relic abundance that is comparable to the measured cosmological dark matter density. And although there are many electroweak processes through which a WIMP could potentially annihilate, none are as ubiquitous across the landscape of dark matter models than those which result from couplings between the dark matter and the Standard Model (SM) Z or Higgs bosons.

As direct detection, indirect detection, and collider searches for dark matter have progressed, the WIMP paradigm has become increasingly well explored and constrained. And although there remain many viable WIMP models, important experimental benchmarks have been reached, providing us with valuable information pertaining to the identity of our universe's dark matter. In this paper, we focus on the subset of models in which the dark matter annihilates through the exchange of the Z or the Higgs boson. In scenarios outside of this subset of models, WIMPs must annihilate through the exchange of particles beyond the SM if they are to avoid being overproduced in the early universe.

The remainder of this article is structured as follows. In Sec. 2, we consider dark matter that is mediated by Z exchange, discussing fermonic, scalar and vector dark matter candidates. We find that nearly all of this parameter space is ruled out by a combination of constraints from direct detection experiments (LUX, PandaX-II) and measurements from LEP of the invisible width of the Z. The only exception to this conclusion is found in the case of a fermonic dark matter candidate with a nearly pure axial coupling to the Z and with a mass that lies within a few GeV of the Z pole ($m_{\rm DM} \simeq 40 - 48$ GeV). As this remaining possibility is expected to be tested in the near future with direct detection experiments such as XENON1T, we will soon have exhaustively explored the class of all Z

mediated dark matter models. In Sec. 3, we consider fermonic, scalar and vector dark matter candidates that are coupled to the SM Higgs boson. Across this class of models, we again find that the overwhelming majority of the parameter space is experimentally excluded, with the exception of scenarios in which the dark matter lies near the Higgs pole ($m_{\rm DM} \simeq m_H/2$), the dark matter is a scalar (vector) heavier than 400 GeV (1160 GeV) with a Higgs portal coupling, or the dark matter is a fermion with largely pseudoscalar couplings to the SM Higgs boson. In Sec. 4 we discuss some caveats to our conclusions, including scenarios with a non-standard cosmological history, or models in which the dark matter coannihilates with another particle species in the early universe. We summarize our results and conclusions in Sec. 5.

2 Z Mediated Dark Matter

2.1 Fermionic dark matter

We begin by considering a dark matter candidate, χ, which is either a Dirac or a Majorana fermion with the following interactions with the SM Z:

$$\mathcal{L} \supset \left[a\bar{\chi}\gamma^{\mu}(g_{\chi v} + g_{\chi a}\gamma^5)\chi\right] Z_{\mu}, \tag{2.1}$$

where $a = 1\,(1/2)$ in the Dirac (Majorana) case, and $g_{\chi v}$ and $g_{\chi a}$ are the vector and axial couplings of the dark matter, respectively. Note that $g_{\chi v}$ is necessarily equal to zero in the Majorana case. These couplings allow the dark matter to annihilate through the s-channel exchange of the Z, into pairs of SM fermions or, if the dark matter is heavy enough, into ZZ, W^+W^- or Zh final states. In Fig. 1 we plot the fraction of annihilations which proceed to each final state, as evaluated in the early universe (at the temperature of thermal freeze-out) and for $v = 10^{-3}\,c$ (as is typically relevant for indirect detection). Throughout this paper, unless otherwise stated, we use version 4.2.5 of the publicly available code MicrOMEGAS [1] to calculate all annihilation cross sections, thermal relic abundances, and elastic scattering cross sections.

In Fig. 2, we explore and summarize the parameter space within this class of models. In each frame, the solid black line represents the value of the dark matter's coupling to the Z ($g_{\chi v}$ or $g_{\chi a}$) for which the calculated thermal relic abundance is equal to the measured cosmological dark matter density, $\Omega_{\chi}h^2 = 0.1198 \pm 0.0015$ [2]. If $m_{\chi} < m_Z/2$, we can further restrict the couplings of the dark matter using the measurement of the invisible Z width. The predicted contribution from Z decays to dark matter is in this case is given by:

$$\Gamma(Z \to \chi\bar{\chi}) = \frac{a\,m_Z}{12\pi}\left(1 - \frac{4m_{\chi}^2}{m_Z^2}\right)^{1/2}\left[g_{\chi a}^2\left(1 - \frac{4m_{\chi}^2}{m_Z^2}\right) + g_{\chi v}^2\left(1 + \frac{2m_{\chi}^2}{m_Z^2}\right)\right], \tag{2.2}$$

where again $a = 1(1/2)$ for dark matter that is a Dirac (Majorana) fermion. In the shaded regions appearing in the upper left corner of each frame of Fig. 2, the predicted invisible width of the Z exceeds the value measured at LEP by more the 2σ, corresponding to a contribution of $\Gamma_Z^{\rm inv} > 1.5$ MeV [3]. Combined with relic abundance considerations, this constraint translates to $m_{\chi} > 25$ GeV (32 GeV) for the case of a purely vector (axial) coupling to the Z.

Direct detection experiments provide a powerful test of dark matter candidates with non-negligible couplings to the Z. After integrating out the Z, the effective interaction

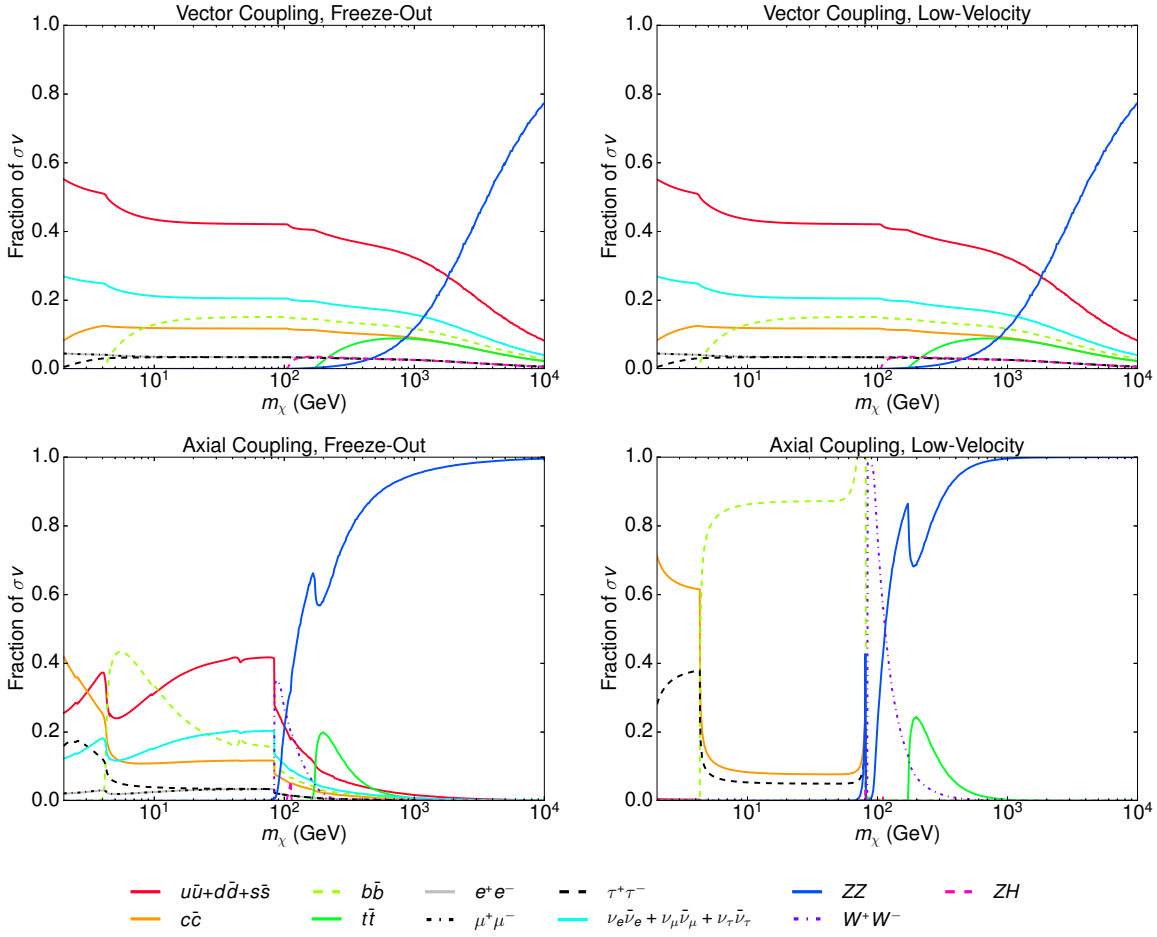

Figure 1. The fraction of dark matter annihilations that proceed to each final state, as evaluated at the temperature of thermal freeze-out (left) and at $v = 10^{-3}\,c$, as is typically relevant for indirect detection (right). The upper and lower frames correspond to dark matter in the form of a fermion with purely vector or purely axial couplings to the Z, respectively.

relevant for dark matter scattering with nuclei is given by:

$$\mathcal{L} = \frac{1}{m_Z^2}\left[\bar{\chi}\gamma^\mu(g_{\chi v} + g_{\chi a}\gamma^5)\chi\right]\left[\bar{q}\gamma^\mu(g_{qv} + g_{qa}\gamma^5)q\right], \tag{2.3}$$

where $g_{uv} = g_2(\frac{1}{4c_W} - \frac{2s_W^2}{3c_W})$, $g_{dv} = g_2(-\frac{1}{4c_W} + \frac{s_W^2}{3c_W})$, $g_{ua} = -g_2/4c_W$, $g_{da} = g_2/4c_W$, etc. are the couplings of the Z to Standard Model quarks.

At low energies, $\bar{\Psi}\gamma^i\Psi \to 0$ and $\bar{\Psi}\gamma^0\gamma^5\Psi \to 0$, and thus only vector-vector and axial-axial interactions are not suppressed by powers of velocity or momentum transfer. These interactions lead to spin-independent and spin-dependent scattering cross sections, respectively. The solid blue curves shown in Fig. 2 represent the current limits on the dark matter's coupling to the Z, as derived from the results of the direct detection experiment LUX [4] (the PandaX-II experiment has placed a constraint that is only slightly weaker [5]).[1]

[1] Although the spin-independent constraints from direct detection experiments are generally presented for

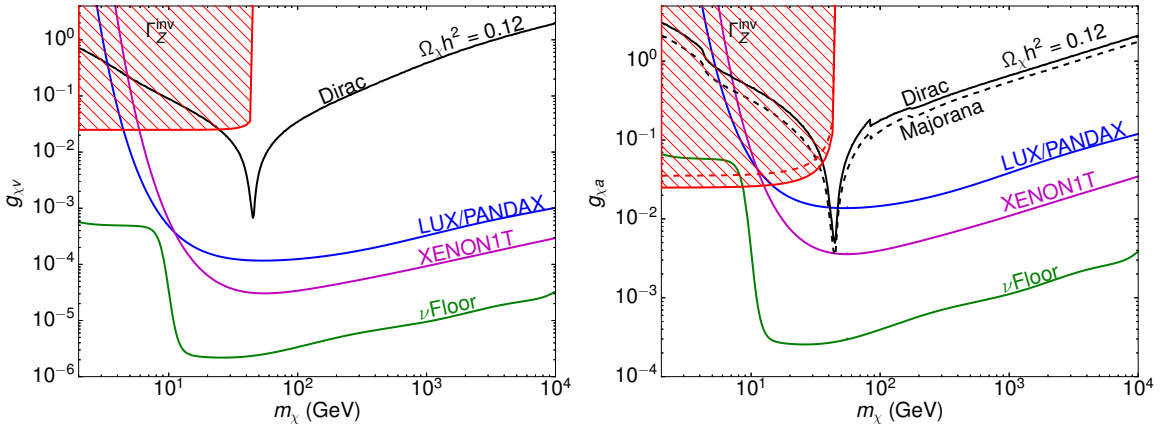

Figure 2. Constraints on the mass and couplings of a fermionic dark matter candidate that annihilates through the Z. The solid black contours indicate the value of the coupling for which the thermal relic abundance matches the measured cosmological dark matter density, $\Omega_\chi h^2 = 0.12$. The shaded regions are excluded by the measurement of the invisible Z width. The left and right frames depict the cases of a purely vector or axial coupling between the dark matter and the Z, respectively. The vast majority of this parameter space is excluded by the current constraints from LUX and PandaX-II [4, 5]. The only currently viable region ($m_\chi = 40 - 48$ GeV with $g_{\chi a} \gg g_{\chi v}$) is expected to be probed in the near future by XENON1T [6].

Together, these constraints rule out the vast majority of the parameter space for fermonic dark matter candidates that annihilate through Z exchange. After accounting for these constraints, we find that an acceptable thermal relic abundance can be obtained only in the near-resonance case ($m_\chi = m_Z/2$) with $g_{\chi a} \gg g_{\chi v}$. Furthermore, we expect that this remaining case will be probed in the near future by direct detection experiments such as XENON1T [6]. It is interesting to note that within the context of the MSSM, a bino-like neutralino (with a subdominant higgsino fraction) can possess the characteristics found within this scenario [7].

In the narrow region of viable parameter space found within this class of models, the dark matter annihilates with a cross section that is chirality suppressed in the low-velocity limit, $\sigma v \propto (m_f/m_\chi)^2$, leading such annihilations to proceed mostly to $b\bar{b}$ final states. In the mass range near the Z-pole, the low-velocity cross section is very sensitive to the value of the dark matter's mass (for analytic expressions of this cross section, see the Appendix of Ref. [13]). In Fig. 3, we plot the effective low-velocity annihilation cross section (as relevant for indirect detection) for fermonic dark matter with an axial coupling to the Z.[2] For masses in the range not yet excluded by LUX or PandaX-II (41-46 GeV or 40-48 GeV for Dirac or

the case of equal couplings to protons and neutrons, we have translated these results to apply to the models at hand. It is interesting to note that a cancellation in the vector couplings of the Z to up and down quarks leads to a suppression in the effective coupling to protons. In particular, Z exchange leads to the following ratio of cross sections with neutrons and protons: $\sigma_n/\sigma_p \approx (2g_{dv} + g_{uv})^2/(2g_{uv} + g_{dv})^2 \approx 180$. We also note that since xenon contains isotopes with an odd number of neutrons (^{129}Xe and ^{131}Xe with abundances of 29.5% and 23.7%, respectively), this target is quite sensitive to spin-dependent WIMP-neutron scattering. To constrain spin-dependent scattering, we converted the results of the most recent spin-independent analysis presented by the LUX collaboration [4].

[2]By "effective" annihilation cross section we denote the value for the case of identical annihilating particles (Majorana fermions). For a Dirac fermion (or a complex boson), the actual particle-antiparticle annihilation cross section is equal to twice this value.

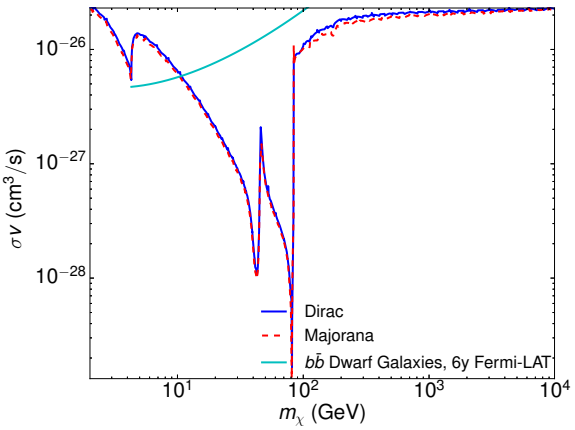

Figure 3. The effective low-velocity annihilation cross section (relevant for indirect detection) for Dirac or Majorana dark matter with an axial coupling to the Z. We note that for the masses in the range not yet excluded by LUX or PandaX-II, this cross section can take on values across the range of $\sigma v \simeq (0.14 - 6.5) \times 10^{-27}$ cm^3/s, below the constraints derived from Fermi and other existing indirect detection experiments [8–12]. We also show the current constraint from Fermi's observation of dwarf spheroidal galaxies [9].

Majorana dark matter, respectively), this cross section can take on values across the range of $\sigma v \simeq (0.14 - 6.5) \times 10^{-27}$ cm^3/s, below the constraints derived from Fermi and other existing indirect detection experiments [8–12]. Within this potentially viable mass range, however, it may be possible for annihilating dark matter to generate the gamma-ray excess observed from the region surrounding the Galactic Center [14–20] (see also Ref. [21]).

2.2 Scalar dark matter

A complex scalar dark matter candidate, ϕ, can couple to the Z through the following interaction:

$$\mathcal{L} \supset i\, g_\phi \phi^\dagger \overleftrightarrow{\partial_\mu} \phi Z^\mu + g_\phi^2 \phi^2 Z^\mu Z_\mu. \tag{2.4}$$

The annihilation cross section to fermion pairs in this case is suppressed by two powers of velocity, and values of g_ϕ that lead to an acceptable thermal relic abundance are shown as a black solid line in the left frame of Fig. 4. We also show in this figure the region of parameter space that is excluded by the measurement of the invisible width of the Z, which receives the following contribution in this case:

$$\Gamma(Z \to \phi\phi^\dagger) = \frac{g_\phi^2 m_Z}{48\pi} \left(1 - \frac{4m_\phi^2}{m_Z^2}\right)^{3/2}. \tag{2.5}$$

In this model, there is an unsuppressed cross section for spin-independent elastic scattering with nuclei, leading to very stringent constraints from LUX and PandaX-II. In the left frame of Fig. 4, we see that the entire parameter space in this scenario is strongly ruled out by a combination of constraints from LUX/PandaX-II and the invisible width of the Z.

2.3 Vector dark matter

An interaction between the Z and a spin-one dark matter candidate, X, can arise at tree-level only through a kinetic term. In this case, gauge invariance requires the interaction to take

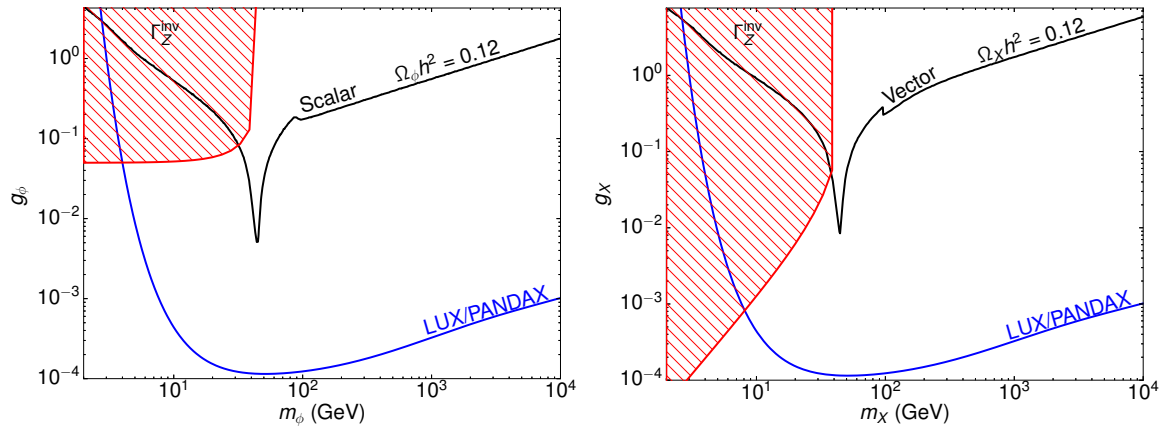

Figure 4. Constraints on mass and couplings of a complex scalar (left frame) or complex vector (right frame) dark matter candidate which annihilates through the Z. The solid black contours indicate the value of the coupling for which the thermal relic abundance matches the measured cosmological dark matter density, $\Omega_\chi h^2 = 0.12$. The shaded regions are excluded by measurements of the invisible Z width, and the regions above the solid blue line are excluded by the current constraints from LUX and PandaX-II [4, 5]. The entire parameter space in each of these scenarios is strongly ruled out.

the following form:

$$\mathcal{L} \supset i\, g_X \left(Z^\mu\, X^{\nu\,\dagger} \partial_{[\mu} X_{\nu]} + X^\dagger_\mu X_\nu\, \partial^\mu Z^\nu \right) + \text{h.c.} \tag{2.6}$$

In the right frame of Fig. 4, we summarize the parameter space in this model. In particular, we apply constraints from the invisible width of the Z, which receives the following contribution in this case:

$$\Gamma(Z \to X X^\dagger) = \frac{g_X^2 m_Z \left(1 - 8 r_{XZ}^2 + 28 r_{XZ}^4 - 48 r_{XZ}^6\right) \left(1 - 4 r_{XZ}^2\right)^{1/2}}{192 \pi r_{XZ}^4}, \tag{2.7}$$

where $r_{XZ} \equiv m_X / m_Z$.

After integrating our the Z, this model yields the following effective interaction for elastic scattering with nuclei (retaining only unsuppressed terms):

$$\mathcal{L}_{\rm eff} \supset \frac{i g_\chi g_{qv}}{m_Z^2} \left(X_\nu \partial_\mu X^{\nu\dagger} \bar{q} \gamma^\mu q + \text{h.c.} \right). \tag{2.8}$$

In the non-relativistic limit, this yields the following WIMP-nucleus cross section:

$$\begin{aligned} \sigma_{\chi N} &= \frac{g_\chi^2 \mu_{\chi N}^2}{\pi m_Z^4} \Big[Z(2 g_{uv} + g_{dv}) + (A - Z)(g_{uv} + 2 g_{dv}) \Big]^2 \\ &\approx \frac{g_\chi^2 (g_1^2 + g_2^2) \mu_{\chi N}^2}{16 \pi m_Z^4} (A - Z)^2, \end{aligned} \tag{2.9}$$

where Z and A are the atomic number and atomic mass of the target nucleus, and $\mu_{\chi N}$ is the reduced mass of the dark matter-nucleus system.

In the right frame of Fig. 4, we see that this combination of constraints from direct detection experiments and the invisible width of the Z strongly rules out the entire parameter space of this model.

3 Higgs Mediated Dark Matter

3.1 Fermionic dark matter

In this subsection, we consider a dark matter candidate that is either a Dirac or Majorana fermion, with the following interactions with the SM Higgs boson:

$$\mathcal{L} \supset \left[a\bar{\chi}(\lambda_{\chi s} + \lambda_{\chi p} i\gamma^5)\chi\right] H, \tag{3.1}$$

where once again $a = 1(1/2)$ in the Dirac (Majorana) case. The quantities $\lambda_{\chi s}$ and $\lambda_{\chi p}$ denote the scalar and pseudoscalar couplings between the dark matter and the SM Higgs, respectively.

Dark matter annihilations in this model depend strongly on the choice of scalar or pseudoscalar couplings. In particular, scalar couplings lead to an annihilation cross section that is suppressed by two powers of velocity, whereas pseudoscalar couplings generate an s-wave amplitude with no such suppression. In both cases, annihilations proceed dominantly to heavy final states (see Fig. 5), due to the couplings of the Higgs to the particle content of the SM.

The contribution to the invisible Higgs width in this case is given by:

$$\Gamma(H \to \chi\bar{\chi}) = \frac{a\, m_H}{8\pi}\left[\lambda_{\chi p}^2 + \lambda_{\chi s}^2\left(1 - \frac{4m_\chi^2}{m_H^2}\right)\right]\sqrt{1 - \frac{4m_\chi^2}{m_H^2}}. \tag{3.2}$$

The current experimental constraint on the invisible branching fraction of the Higgs is $\Gamma_{\rm inv}/(\Gamma_{\rm inv} + \Gamma_{SM}) < 0.24$,[3] which for $\Gamma_{SM}^H \approx 4.07\,\text{MeV}$ corresponds to the following:

$$\Gamma(H \to \chi\bar{\chi}) < \Gamma_{SM}^H \frac{\text{BR}(H \to \text{inv})}{1 - \text{BR}(H \to \text{inv})} \approx 1.29\,\text{MeV}. \tag{3.3}$$

Elastic scattering between dark matter and nuclei is entirely spin-independent in this case, with a cross section given as follows:

$$\sigma_{\chi N} \approx \frac{\mu_{\chi N}^2}{\pi m_H^4}\left[Z f_p + (A - Z) f_n\right]^2 \left[\lambda_{\chi s}^2 + \lambda_{\chi p}^2 \frac{q^2}{4m_\chi^2}\right], \tag{3.4}$$

where q is the momentum exchanged in the collision.

In Fig. 6, we summarize the constraints on this scenario. In the case of a purely scalar coupling ($\lambda_{\chi p} = 0$, shown in the left frame), the combination of the invisible Higgs width measurement and the results of direct detection experiments rule out nearly all of the parameter space. The exception is the mass range within a few GeV of the Higgs pole, $m_\chi =$ 56-62 GeV. In this case, future experiments such as XENON1T are expected to test the remaining region of parameter space.

In the case of a purely pseudoscalar coupling ($\lambda_{\chi s} = 0$, shown in the right frame of Fig. 6), the momentum suppression of the elastic scattering cross section strongly reduces the prospects for direct detection experiments, earning this scenario the moniker of "coy dark matter" [22–24]. Naively, we expect the sensitivity of direct detection experiments to

[3] This is derived from a combination of Run I and 2015 LHC data. See, for example, page 25 of the talk "Search for invisible decays of the 125 GeV Higgs boson using the CMS detector", by Nicholas Wardle, http://indico.cern.ch/event/432527/contributions/1071583/attachments/1320936/1980904/nckw_ICHEP_2016_hinv_cms.pdf.

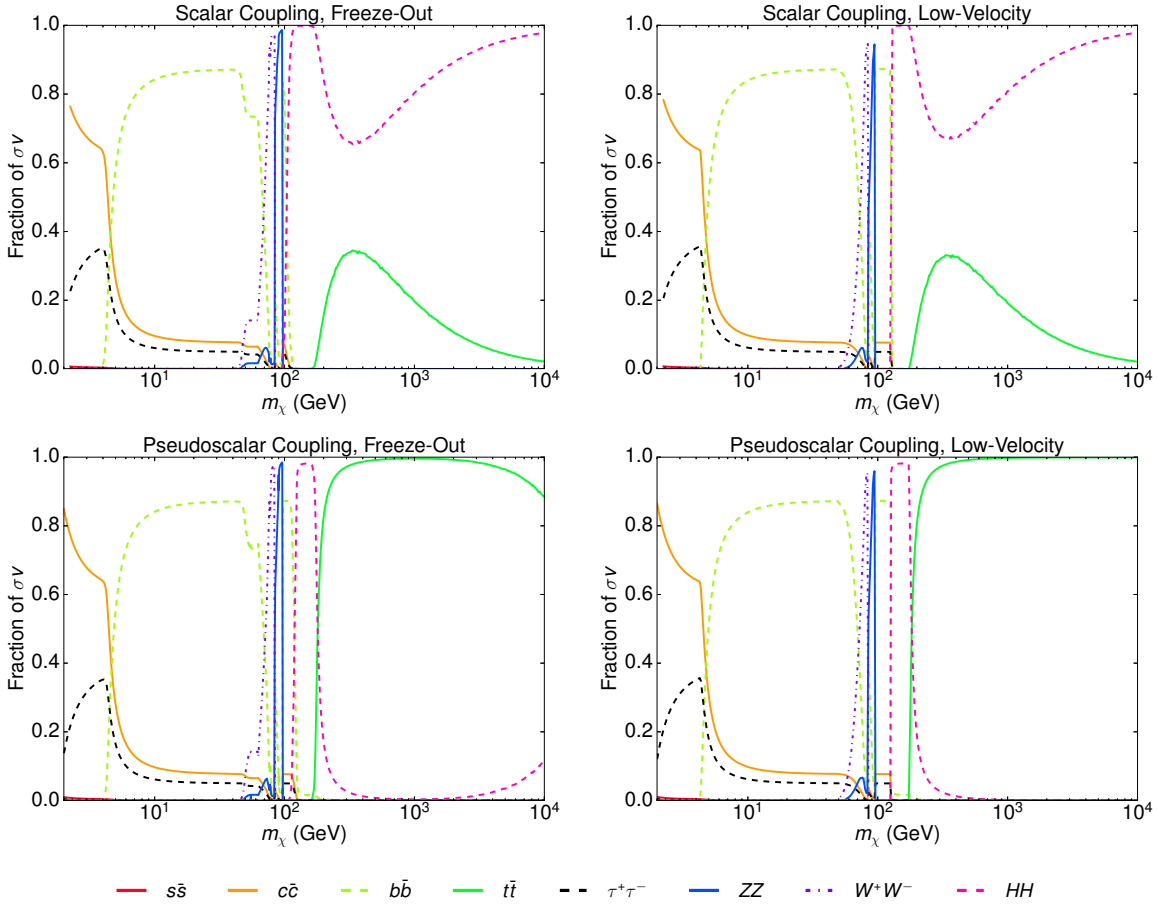

Figure 5. The fraction of dark matter annihilations that proceed to each final state, as evaluated at the temperature of thermal freeze-out (left) and at $v = 10^{-3}\,c$, as is typically relevant for indirect detection (right). The upper and lower frames correspond to dark matter in the form of a fermion with purely scalar or purely pseudoscalar couplings to the Standard Model Higgs boson, respectively.

the coupling, $\lambda_{\chi p}$, to be suppressed relative to $\lambda_{\chi s}$ by a factor of $q/2m_\chi$, which for typical scattering events is on the order of 10^{-3}. Simply rescaling the results shown in the left frame of Fig. 6 by this factor leads us to conclude that current (LUX, PandaX-II) and near future (XENON1T) experiments will not be sensitive to dark matter in this scenario. It is less clear, however, whether a larger experiment, with a sensitivity to cross sections near the neutrino floor, might be sensitive to this scenario. With this in mind, we have calculated the sensitivity of such an experiment to a dark matter candidate with a momentum suppressed elastic scattering cross section with nuclei.

Dark matter with velocity or momentum suppressed scattering has been considered previously in the literature (see, for example, Refs. [25–34]). To compute the number of events in a large volume xenon experiment, we follow the procedure outlined in Ref. [34], adopting a standard Maxwellian velocity distribution ($v_0 = 220$ km/s, $v_{\rm esc} = 544$ km/s, $\bar{v}_{\rm Earth} = 245$ km/s), a local density of $0.3\,{\rm GeV/cm^3}$, and a Helm form factor [35]. Regarding the detector specifications, we assume an optimistic scenario with an energy independent efficiency of 25% and perfect energy resolution. We consider events with nuclear recoil energies between 6 and

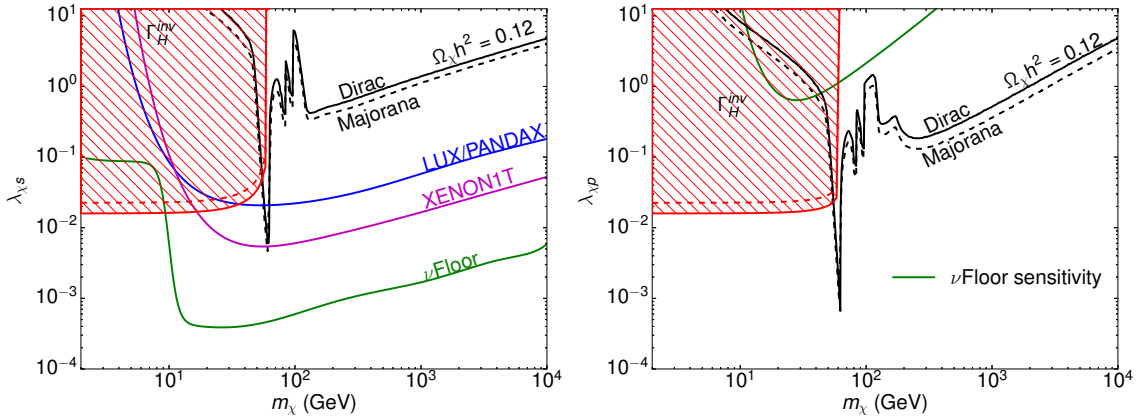

Figure 6. Constraints on mass and couplings of a fermionic dark matter candidate which annihilates through the Standard Model Higgs boson. The solid black contours indicate the value of the coupling for which the thermal relic abundance matches the measured cosmological dark matter density, $\Omega_\chi h^2 = 0.12$. The shaded regions are excluded by measurements of the invisible Higgs width. The left and right frames depict the cases of a purely scalar or pseudoscalar coupling between the dark matter and the Higgs, respectively. In the scalar case, the vast majority of this parameter space is excluded by the current constraints from LUX and PandaX-II [4, 5]. The only currently viable region ($m_\chi =$ 56-62 GeV is expected to be probed in the near future by XENON1T [6]. Due to the momentum suppression of the elastic scattering cross section, the case of dark matter with a pseudoscalar coupling to the Higgs is much less strongly constrained.

30 keV, where this lower limits was imposed in order to reduce the rate of neutrino-induced background events [36, 37]. From the calculated event rate, we apply Poisson statistics to place a 90% confidence level constraint on the dark matter coupling, assuming that zero events are observed. In the right frame of Fig. 6, we plot the projected constraint from such an experiment after collecting an exposure of 30 ton-years, which is approximately the exposure that we estimate will accumulate between ∼1-3 neutrino-induced background events. From this, we conclude that even with such an idealized detector, it will not be possible to test a dark matter candidate with a purely pseudoscalar coupling to the Higgs.

In the case of dark matter with a scalar coupling and near the Higgs pole, the low-velocity annihilation cross section is suppressed by two powers of velocity, making such a scenario well beyond the reach of any planned or proposed indirect detection experiment (see the left frame of Fig. 7). In the case of dark matter with a pseudoscalar coupling to the Higgs, however, the low-velocity annihilation rate is unsuppressed, leading to more promising prospects for indirect detection (for analytic expressions of these cross section, see the Appendix of Ref. [13]). In the right frame of Fig. 7, we plot the low-velocity annihilation cross section (as relevant for indirect detection) for fermonic (Dirac or Majorana) dark matter with a pseudoscalar coupling to the SM Higgs boson. In this case, constraints from Fermi's observations of dwarf spheroidal galaxies [9] may be relevant, depending on the precise value of the dark matter mass. We also note that uncertainties associated with the distribution of dark matter in these systems could plausibly weaken these constraints to some degree [38–41]. It may also be possible in this scenario [22, 42–44] to generate the gamma-ray excess observed from the region surrounding the Galactic Center [14–20].

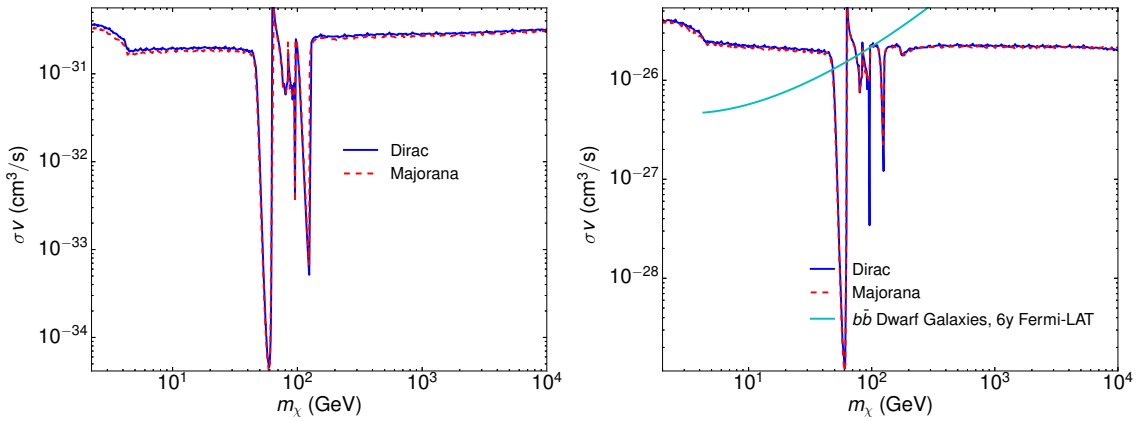

Figure 7. The effective low-velocity annihilation cross section (relevant for indirect detection) for Dirac or Majorana dark matter with a scalar (left) or pseudoscalar (right) coupling to the SM Higgs boson. For the case of scalar couplings, the cross section is always well below the sensitivity of Fermi and other existing indirect detection experiments. In the pseudoscalar case, the prospects for indirect detection are much more encouraging. In the right frame, we also show the current constraint from Fermi's observation of dwarf spheroidal galaxies [9].

3.2 Scalar dark matter

In the case of scalar dark matter with a coupling to the SM Higgs boson, we consider a Higgs Portal interaction, described by the following Lagrangian:

$$\mathcal{L} \supset a\,\lambda_{\phi H}\left[vH\phi^2 + \frac{1}{2}H^2\phi^2\right], \tag{3.5}$$

where $a = 1\,(1/2)$ in the case of a complex (real) scalar, and v is the vacuum expectation value of the SM Higgs boson.

In this class of models, the dark matter annihilates without velocity suppression, and preferentially to heavy final states (see Fig. 8). The contribution to the invisible Higgs width in this case is given by:

$$\Gamma(H \to \phi\phi^\dagger) = \frac{a\,v^2\lambda_{\phi H}^2}{16\,\pi m_H}\sqrt{1-\frac{4m_\phi^2}{m_H^2}}. \tag{3.6}$$

In Fig. 9, we plot a summary of the constraints in this class of models. In this case, we find that complex (real) scalar dark matter with a mass greater than 840 GeV (400 GeV) is not currently constrained, along with the region near the Higgs pole. XENON1T is expected to probe the remaining high mass window up to 10 TeV (5 TeV).

In Fig. 10, we plot the low-velocity annihilation cross section (as relevant for indirect detection) for scalar dark matter with a Higgs portal coupling. In the currently allowed mass range near the Higgs pole, this class of models predicts a very small low-velocity annihilation cross section, which is likely unable to generate the measured intensity of the Galactic Center gamma-ray excess [14–20] (see also, Refs. [45, 46]).

3.3 Vector dark matter

In the case of vector dark matter, we again consider a Higgs Portal interaction, which is described in this case by the following Lagrangian:

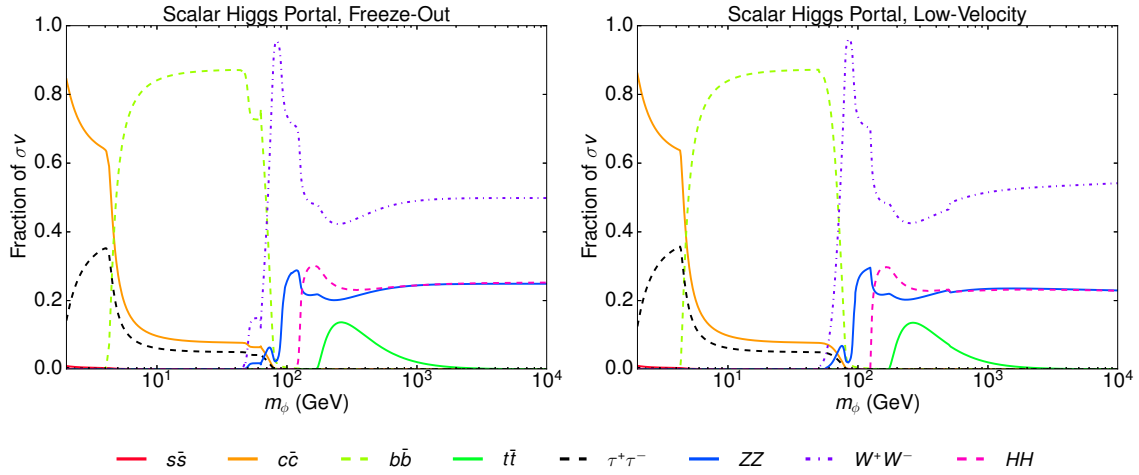

Figure 8. The fraction of dark matter annihilations that proceed to each final state, as evaluated at the temperature of thermal freeze-out (left) and at $v = 10^{-3}\,c$, as is typically relevant for indirect detection (right), for the case of scalar dark matter coupled to the Standard Model Higgs boson.

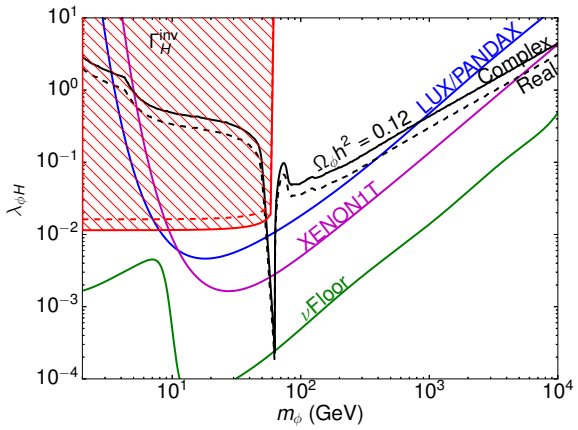

Figure 9. Constraints on mass and couplings of a complex scalar dark matter candidate which annihilates through a Higgs portal coupling. The solid black contour indicates the value of the coupling for which the thermal relic abundance matches the measured cosmological dark matter density, $\Omega_\chi h^2 = 0.12$. The shaded region is excluded by measurements of the invisible Higgs width, and the region above the solid blue line is excluded by the current constraints from LUX and PandaX-II [4, 5]. This scenario is currently viable only if the mass of the dark matter candidate is near the Higgs pole ($m \simeq m_H/2$) or if $m_\phi \gtrsim 400$ GeV.

$$\mathcal{L} \supset a\lambda_{XH}\left[vHX^\mu X_\mu^\dagger + \frac{1}{2}H^2 X^\mu X_\mu^\dagger\right], \tag{3.7}$$

where $a = 1\,(1/2)$ in the case of a complex (real) vector. As in the cases considered in the previous subsection, dark matter annihilates without velocity suppression in this class of models, and preferentially to heavy final states (see Fig. 11).

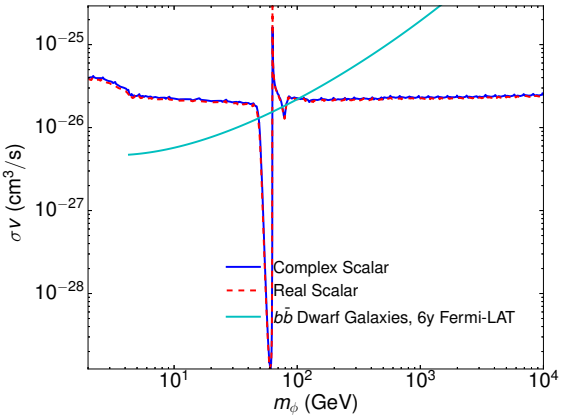

Figure 10. The effective low-velocity annihilation cross section (relevant for indirect detection) for complex or real scalar dark matter with a Higgs portal coupling. We also show the current constraint from Fermi's observation of dwarf spheroidal galaxies [9].

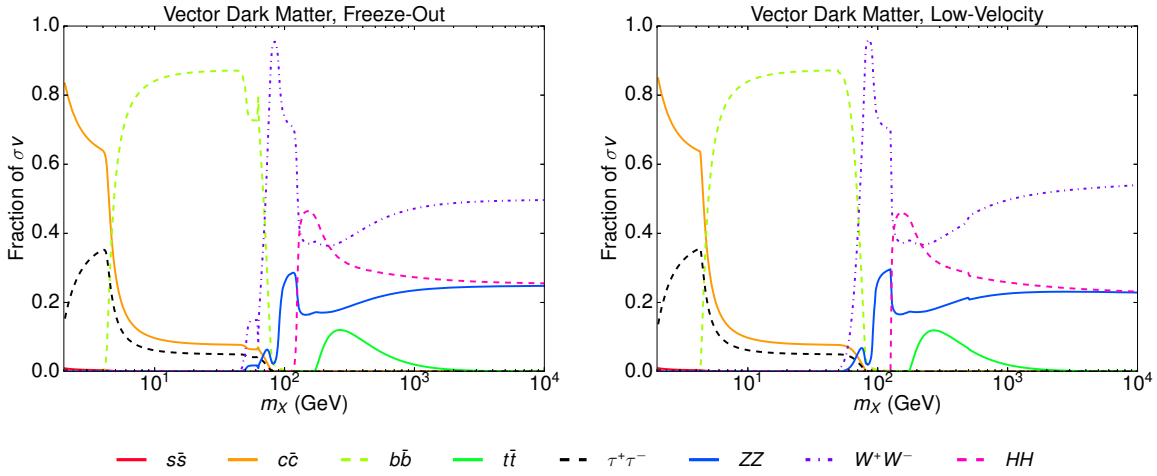

Figure 11. The fraction of dark matter annihilations that proceed to each final state, as evaluated at the temperature of thermal freeze-out (left) and at $v = 10^{-3}\,c$, as is typically relevant for indirect detection (right), for the case of dark matter in the form of a vector which annihilates through its coupling to the Standard Model Higgs boson.

The contribution to the invisible Higgs width is given in this model by:

$$\Gamma(H \to XX^\dagger) = \frac{a\,\lambda_{XH}^2 v^2 m_H^3}{64\pi m_X^4}\left(1 - 4\frac{m_X^2}{m_H^2} + 12\frac{m_X^4}{m_H^4}\right)\sqrt{1 - \frac{4m_X^2}{m_H^2}}. \tag{3.8}$$

The constraints on this scenario are summarized in Fig. 12. The combination of constraints from LUX/PandaX-II and on the invisible Higgs width rule out all of the parameter space in this class of models, with the exception of the mass range near the Higgs pole, $m_X \simeq m_H/2$ or for $m_X \gtrsim 1160$ GeV. XENON1T is expected in the near future to probe most of this remaining high mass window, covering nearly the entire range of perturbative values for the coupling, $\lambda_{XH} \lesssim 4\pi$.

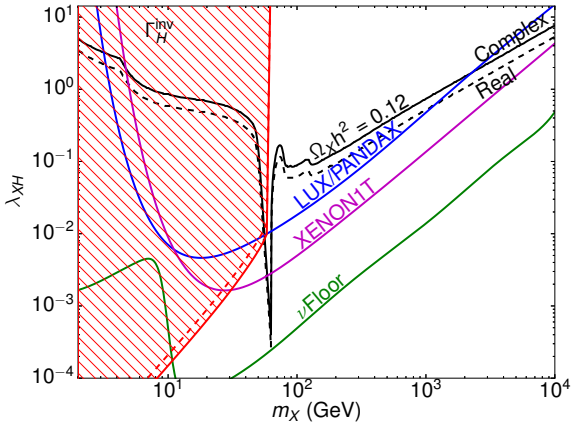

Figure 12. Constraints on mass and couplings of a complex vector dark matter candidate which annihilates through the Standard Model Higgs boson. The solid black contour indicates the value of the coupling for which the thermal relic abundance matches the measured cosmological dark matter density, $\Omega_\chi h^2 = 0.12$. The shaded region is excluded by measurements of the invisible Higgs width, and the region above the solid blue line is excluded by the current constraints from LUX and PandaX-II [4, 5]. This scenario is currently viable only if the mass of the dark matter candidate is near the Higgs pole ($m \simeq m_H/2$) or if $m_X \gtrsim 1160$ GeV.

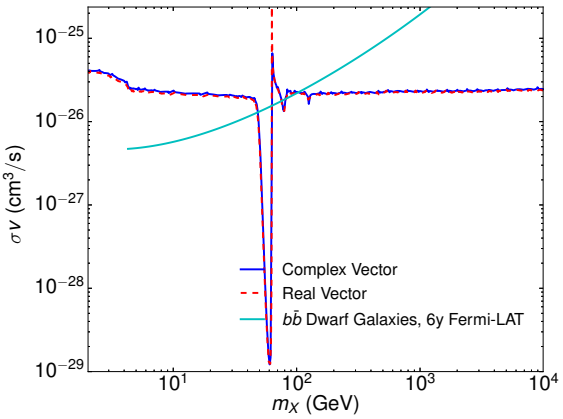

Figure 13. The effective low-velocity annihilation cross section (relevant for indirect detection) for complex or real vector dark matter with a coupling to the Standard Model Higgs boson. We also show the current constraint from Fermi's observation of dwarf spheroidal galaxies [9].

We plot in Fig. 13 the low-velocity annihilation cross section (as relevant for indirect detection) in this class of models, along with the constraints from Fermi's observations of dwarf spheroidal galaxies [9]. In the currently allowed mass range near the Higgs pole, this class of models predicts a very small low-velocity annihilation cross section, which is likely unable to generate the measured intensity of the Galactic Center gamma-ray excess [14–20].

4 Caveats

The conclusions presented here rely on a number of assumptions that we have implicitly made throughout this study. In particular, we have assumed that the thermal history of the early universe is well described by the standard radiation-dominated picture. Departures from this simple thermal history could potentially reduce the couplings of the dark matter that are required to generate an acceptable thermal relic abundance, thereby relaxing the constraints from direct detection experiments and from measurements of the invisible Z and Higgs widths. Examples of such scenarios include those in which the abundance of dark matter is depleted as a result of an out-of-equilibrium decay [47–53] or a period of late-time inflation [54–58].

We have also limited our analysis in this paper to couplings between pairs of dark matter particles and one or more Z or Higgs bosons. We could instead have considered couplings between one dark matter particle, the Z or Higgs, and an additional state. If the additional state is not much heavier than the dark matter itself, such a coupling could allow the dark matter to be depleted in the early universe through coannihilations [59, 60], without necessarily inducing a large elastic scattering cross section with nuclei. Generally speaking, if such coannihilations are to be efficient, such states must have a mass that is within roughly $\sim$10% of the mass of the dark matter particle itself.

Phenomenology of this kind can be easily realized if we consider a Dirac fermion that is split into a pair of nearly degenerate Majorana fermions by a small Majorana mass term. Following Refs. [61, 62], the Lagrangian in this scenario takes the following form:

$$\begin{aligned}\mathcal{L} \supset\; & \frac{1}{2}\bar{\Psi}_1 i\gamma^\mu\partial_\mu\Psi_1 - \frac{1}{2}(M-m_+)\bar{\Psi}_1\Psi_1 + \frac{1}{2}\bar{\Psi}_2 i\gamma^\mu\partial_\mu\Psi_2 - \frac{1}{2}(M+m_+)\bar{\Psi}_2\Psi_2 \\ & + i\,g\,Q\,Z_\mu\,\bar{\Psi}_2\gamma_\mu\Psi_1 + \frac{1}{2}\,g\,Q\,Z_\mu\,\frac{m_-}{M}\,\left(\bar{\Psi}_2\gamma^\mu\gamma^5\Psi_2 - \bar{\Psi}_1\gamma^\mu\gamma^5\Psi_1\right) + \mathcal{O}\left(\frac{m^2}{M^2}\right),\end{aligned} \tag{4.1}$$

where Ψ_1 and Ψ_2 are the two quasi-degenerate Majorana fermions, $m_\pm = (m_L \pm m_R)/2$, and $M \gg m_{L,R}$. Setting $m_R = 0$, this reduces to

$$\begin{aligned}\mathcal{L} \supset\; & \frac{1}{2}\bar{\Psi}_1 i\gamma^\mu\partial_\mu\Psi_1 - \frac{1}{2}M_1\bar{\Psi}_1\Psi_1 + \frac{1}{2}\bar{\Psi}_2 i\gamma^\mu\partial_\mu\Psi_2 - \frac{1}{2}M_2\bar{\Psi}_2\Psi_2 \\ & + i\,g_{cv}\,Z_\mu\,\bar{\Psi}_2\gamma_\mu\Psi_1 + \frac{1}{2}g_{cv}\,Z_\mu\,\frac{M_1-M_2}{M_1+M_2}\,\left(\bar{\Psi}_2\gamma^\mu\gamma^5\Psi_2 - \bar{\Psi}_1\gamma^\mu\gamma^5\Psi_1\right) + \mathcal{O}\left(\frac{M_1-M_2}{M_1+M_2}\right)^2,\end{aligned}$$

where the $M_1 = M - m_+$ and $M_2 = M + m_+$ are the masses of the lighter and heavier Majorana fermions, respectively. As a result of this mass splitting, all couplings between two of the same Majorana fermion and the Z are suppressed by a factor of $|M_1 - M_2|/(M_1 + M_2) = m_+/M$, strongly limiting the rates of both self-annihilation and elastic scattering with nuclei. In contrast, interactions between the two different Majorana states, $\Psi_1\,\Psi_2$, and the Z are not suppressed, potentially allowing for coannihilations to efficiently deplete their abundances in the early universe.

5 Summary and Conclusions

In this study, we have systematically considered dark matter models which annihilate through couplings to the Standard Model Z or Higgs boson. Overall, we find that the vast majority of the parameter space associated with these models is ruled out by a combination of direct

Dark Matter	Z, Higgs Coupling	Direct	Status	XENON1T	Indirect (10^{-26} cm^3/s)
Majorana Fermion	$\chi\gamma^\mu\gamma^5\chi Z_\mu$	$\sigma_{SD} \sim 1$	$m_\chi \sim m_Z/2$	Yes	$\sigma v \simeq 0.014 - 0.65$
Dirac Fermion	$\bar{\chi}\gamma^\mu\chi Z_\mu$	$\sigma_{SI} \sim 1$	Excluded	–	–
Dirac Fermion	$\bar{\chi}\gamma^\mu\gamma^5\chi Z_\mu$	$\sigma_{SD} \sim 1$	$m_\chi \sim m_Z/2$	Yes	$\sigma v \simeq 0.014 - 0.65$
Complex Scalar	$\phi^\dagger \overleftrightarrow{\partial_\mu} \phi Z^\mu$, $\phi^2 Z^\mu Z_\mu$	$\sigma_{SI} \sim 1$	Excluded	–	–
Complex Vector	$(X^\dagger_\nu \partial_\mu X^\nu + \text{h.c.})\text{Z}^\mu$	$\sigma_{SI} \sim 1$	Excluded	–	–
Majorana Fermion	$\chi\chi H$	$\sigma_{SI} \sim 1$	$m_\chi \sim m_H/2$	Yes	$\sigma v \simeq$ small
Majorana Fermion	$\chi\gamma^5\chi H$	$\sigma_{SI} \sim q^2$	$m_\chi \gtrsim 54$ GeV	No	$\sigma v \simeq 0.0011 - 3.4$
Dirac Fermion	$\bar{\chi}\chi H$	$\sigma_{SI} \sim 1$	$m_\chi \sim m_H/2$	Yes	$\sigma v \simeq$small
Dirac Fermion	$\bar{\chi}\gamma^5\chi H$	$\sigma_{SI} \sim q^2$	$m_\chi \gtrsim 56$ GeV	No	$\sigma v \simeq 0.0012 - 1.7$
Real Scalar	$\phi^2 H^2$	$\sigma_{SI} \sim 1$	$m_\chi \sim m_H/2$ or $m_\chi \gtrsim 400$ GeV	Maybe Up to 5 TeV	$\sigma v \simeq 0.0012 - 0.019$ $\sigma v \simeq 2.1 - 2.3$
Complex Scalar	$\phi^2 H^2$	$\sigma_{SI} \sim 1$	$m_\chi \sim m_H/2$ or $m_\chi \gtrsim 840$ GeV	Maybe Up to 10 TeV	$\sigma v \simeq 0.0019 - 0.017$ $\sigma v \simeq 2.1 - 2.3$
Real Vector	$X_\mu X^\mu H^2$	$\sigma_{SI} \sim 1$	$m_\chi \sim m_H/2$ or $m_\chi \gtrsim 1160$ GeV	Maybe Up to 15 TeV	$\sigma v \simeq 0.0018 - 0.022$ $\sigma v \simeq 2.1 - 2.3$
Complex Vector	$X^\dagger_\mu X^\mu H^2$	$\sigma_{SI} \sim 1$	$m_\chi \sim m_H/2$ or $m_\chi \gtrsim 2200$ GeV	Maybe Yes	$\sigma v \simeq 0.0012 - 0.0064$ $\sigma v \simeq 2.1 - 2.3$

Table 1. A summary of the various classes of dark matter models that we have considered in this study. For each case, we list (in the column labeled "Status") the range of masses (if any) that is not currently excluded experimentally. For those cases which are not already excluded, we state whether XENON1T is anticipated to be sensitive to that model. We also present the range of low-velocity annihilation cross sections that can be found in each case for masses within the currently acceptable range.

detection experiments (LUX, PandaX-II, etc.) and measurements at colliders of the invisible Z and Higgs widths. If no detection is made, we expect experiments such as XENON1T to entirely rule out all remaining Z mediated models in the near future. Such experiments are also expected to test all remaining Higgs mediated models, with the exception of scalar or vector dark matter with masses very near the Higgs annihilation resonance ($m_{\rm DM} \simeq m_H/2$) or fermonic dark matter with a pseudoscalar (CP violating) coupling to the Standard Model Higgs boson. Very heavy dark matter with a large Higgs portal coupling ($\lambda_{\phi H}, \lambda_{XH} \gg 1$) may also be beyond the reach of XENON1T, although LUX-ZEPLIN and other planned experiments will be able to probe such models.

In Table 1, we summarize the various classes of dark matter models that we have considered in this study, listing in each case the range of masses (if any) that is not currently excluded experimentally. For those cases that are not already excluded, we list whether XENON1T is expected to have the sensitivity required to test each class of model. We also present the range of low-velocity annihilation cross sections that can be found within the currently acceptable mass range. For those models with roughly $\sigma v \gtrsim 3 \times 10^{-27}$ cm^3/s (corresponding to $\sigma v \gtrsim 0.3$ in the units used in the Table), the Galactic Center gamma-ray excess could plausibly be generated though dark matter annihilations.

Acknowledgments. ME is supported by the Spanish FPU13/03111 grant of MECD and also by the European projects H2020-MSCA-RISE-2015 and H2020-MSCA-ITN-2015/674896-ELUSIVES. AB is supported by the Kavli Institute for cosmological physics at the University of Chicago through grant NSF PHY-1125897. DH is supported by the US Department of Energy under contract DE-FG02-13ER41958. Fermilab is operated by Fermi Research Al-

liance, LLC, under Contract No. DE-AC02-07CH11359 with the US Department of Energy. This work was carried out in part at the Aspen Center for Physics, which is supported by National Science Foundation grant PHY-1066293.

References

[1] G. Blanger, F. Boudjema, A. Pukhov and A. Semenov, *micrOMEGAs4.1: two dark matter candidates*, *Comput. Phys. Commun.* **192** (2015) 322–329, [1407.6129].

[2] Planck collaboration, P. A. R. Ade et al., *Planck 2015 results. XIII. Cosmological parameters*, 1502.01589.

[3] Particle Data Group collaboration, K. A. Olive et al., *Review of Particle Physics*, *Chin. Phys.* **C38** (2014) 090001.

[4] D. S. Akerib et al., *Results from a search for dark matter in LUX with 332 live days of exposure*, 1608.07648.

[5] PandaX-II collaboration, A. Tan et al., *Dark Matter Results from First 98.7-day Data of PandaX-II Experiment*, 1607.07400.

[6] XENON collaboration, E. Aprile et al., *Physics reach of the XENON1T dark matter experiment*, *JCAP* **1604** (2016) 027, [1512.07501].

[7] D. Hooper, C. Kelso, P. Sandick and W. Xue, *Closing Supersymmetric Resonance Regions With Direct Detection Experiments*, *Phys. Rev.* **D88** (2013) 015010, [1304.2417].

[8] D. Hooper, C. Kelso and F. S. Queiroz, *Stringent and Robust Constraints on the Dark Matter Annihilation Cross Section From the Region of the Galactic Center*, *Astropart. Phys.* **46** (2013) 55–70, [1209.3015].

[9] Fermi-LAT collaboration, M. Ackermann et al., *Searching for Dark Matter Annihilation from Milky Way Dwarf Spheroidal Galaxies with Six Years of Fermi Large Area Telescope Data*, *Phys. Rev. Lett.* **115** (2015) 231301, [1503.02641].

[10] L. Bergstrom, T. Bringmann, I. Cholis, D. Hooper and C. Weniger, *New limits on dark matter annihilation from AMS cosmic ray positron data*, *Phys. Rev. Lett.* **111** (2013) 171101, [1306.3983].

[11] G. Giesen, M. Boudaud, Y. Gnolini, V. Poulin, M. Cirelli, P. Salati et al., *AMS-02 antiprotons, at last! Secondary astrophysical component and immediate implications for Dark Matter*, *JCAP* **1509** (2015) 023, [1504.04276].

[12] M. Cirelli and G. Giesen, *Antiprotons from Dark Matter: Current constraints and future sensitivities*, *JCAP* **1304** (2013) 015, [1301.7079].

[13] A. Berlin, D. Hooper and S. D. McDermott, *Simplified Dark Matter Models for the Galactic Center Gamma-Ray Excess*, *Phys. Rev.* **D89** (2014) 115022, [1404.0022].

[14] T. Daylan, D. P. Finkbeiner, D. Hooper, T. Linden, S. K. N. Portillo, N. L. Rodd et al., *The characterization of the gamma-ray signal from the central Milky Way: A case for annihilating dark matter*, *Phys. Dark Univ.* **12** (2016) 1–23, [1402.6703].

[15] D. Hooper and L. Goodenough, *Dark Matter Annihilation in The Galactic Center As Seen by the Fermi Gamma Ray Space Telescope*, *Phys.Lett.* **B697** (2011) 412–428, [1010.2752].

[16] D. Hooper and T. Linden, *On The Origin Of The Gamma Rays From The Galactic Center*, *Phys.Rev.* **D84** (2011) 123005, [1110.0006].

[17] L. Goodenough and D. Hooper, *Possible Evidence For Dark Matter Annihilation In The Inner Milky Way From The Fermi Gamma Ray Space Telescope*, 0910.2998.

[18] K. N. Abazajian and M. Kaplinghat, *Detection of a Gamma-Ray Source in the Galactic Center Consistent with Extended Emission from Dark Matter Annihilation and Concentrated Astrophysical Emission*, *Phys.Rev.* **D86** (2012) 083511, [1207.6047].

[19] C. Gordon and O. Macias, *Dark Matter and Pulsar Model Constraints from Galactic Center Fermi-LAT Gamma Ray Observations*, *Phys.Rev.* **D88** (2013) 083521, [1306.5725].

[20] Fermi-LAT collaboration, M. Ajello et al., *Fermi-LAT Observations of High-Energy γ-Ray Emission Toward the Galactic Center*, *Astrophys. J.* **819** (2016) 44, [1511.02938].

[21] G. Arcadi, Y. Mambrini and F. Richard, *Z-portal dark matter*, *JCAP* **1503** (2015) 018, [1411.2985].

[22] C. Boehm, M. J. Dolan, C. McCabe, M. Spannowsky and C. J. Wallace, *Extended gamma-ray emission from Coy Dark Matter*, *JCAP* **1405** (2014) 009, [1401.6458].

[23] A. Hektor and L. Marzola, *Coy Dark Matter and the anomalous magnetic moment*, *Phys. Rev.* **D90** (2014) 053007, [1403.3401].

[24] J. Kozaczuk and T. A. W. Martin, *Extending LHC Coverage to Light Pseudoscalar Mediators and Coy Dark Sectors*, *JHEP* **04** (2015) 046, [1501.07275].

[25] S. Chang, A. Pierce and N. Weiner, *Momentum Dependent Dark Matter Scattering*, *JCAP* **1001** (2010) 006, [0908.3192].

[26] B. Feldstein, A. L. Fitzpatrick and E. Katz, *Form Factor Dark Matter*, *JCAP* **1001** (2010) 020, [0908.2991].

[27] S. Chang, A. Pierce and N. Weiner, *Using the Energy Spectrum at DAMA/LIBRA to Probe Light Dark Matter*, *Phys. Rev.* **D79** (2009) 115011, [0808.0196].

[28] K. R. Dienes, J. Kumar, B. Thomas and D. Yaylali, *Overcoming Velocity Suppression in Dark-Matter Direct-Detection Experiments*, *Phys. Rev.* **D90** (2014) 015012, [1312.7772].

[29] J. Fan, M. Reece and L.-T. Wang, *Non-relativistic effective theory of dark matter direct detection*, *JCAP* **1011** (2010) 042, [1008.1591].

[30] J. B. Dent, B. Dutta, J. L. Newstead and L. E. Strigari, *Effective field theory treatment of the neutrino background in direct dark matter detection experiments*, *Phys. Rev.* **D93** (2016) 075018, [1602.05300].

[31] A. Beniwal, F. Rajec, C. Savage, P. Scott, C. Weniger, M. White et al., *Combined analysis of effective Higgs portal dark matter models*, *Phys. Rev.* **D93** (2016) 115016, [1512.06458].

[32] V. Gluscevic, M. I. Gresham, S. D. McDermott, A. H. G. Peter and K. M. Zurek, *Identifying the Theory of Dark Matter with Direct Detection*, *JCAP* **1512** (2015) 057, [1506.04454].

[33] J. Kumar and D. Marfatia, *Matrix element analyses of dark matter scattering and annihilation*, *Phys. Rev.* **D88** (2013) 014035, [1305.1611].

[34] C. Savage, G. Gelmini, P. Gondolo and K. Freese, *Compatibility of DAMA/LIBRA dark matter detection with other searches*, *JCAP* **0904** (2009) 010, [0808.3607].

[35] J. D. Lewin and P. F. Smith, *Review of mathematics, numerical factors, and corrections for dark matter experiments based on elastic nuclear recoil*, *Astropart. Phys.* **6** (1996) 87–112.

[36] J. Billard, L. Strigari and E. Figueroa-Feliciano, *Implication of neutrino backgrounds on the reach of next generation dark matter direct detection experiments*, *Phys. Rev.* **D89** (2014) 023524, [1307.5458].

[37] LZ collaboration, D. S. Akerib et al., *LUX-ZEPLIN (LZ) Conceptual Design Report*, 1509.02910.

[38] V. Bonnivard, C. Combet, D. Maurin and M. G. Walker, *Spherical Jeans analysis for dark matter indirect detection in dwarf spheroidal galaxies - Impact of physical parameters and*

triaxiality, *Mon. Not. Roy. Astron. Soc.* **446** (2015) 3002–3021, [1407.7822].

[39] V. Bonnivard, D. Maurin and M. G. Walker, *Contamination of stellar-kinematic samples and uncertainty about dark matter annihilation profiles in ultrafaint dwarf galaxies: the example of Segue I*, *Mon. Not. Roy. Astron. Soc.* **462** (2016) 223–234, [1506.08209].

[40] K. Ichikawa, M. N. Ishigaki, S. Matsumoto, M. Ibe, H. Sugai and K. Hayashi, *Foreground effect on the J-factor estimation of classical dwarf spheroidal galaxies*, 1608.01749.

[41] N. Klop, F. Zandanel, K. Hayashi and S. Ando, *Impact of axisymmetric mass models for dwarf spheroidal galaxies on indirect dark matter searches*, 1609.03509.

[42] A. Berlin, S. Gori, T. Lin and L.-T. Wang, *Pseudoscalar Portal Dark Matter*, *Phys. Rev.* **D92** (2015) 015005, [1502.06000].

[43] S. Ipek, D. McKeen and A. E. Nelson, *A Renormalizable Model for the Galactic Center Gamma Ray Excess from Dark Matter Annihilation*, *Phys. Rev.* **D90** (2014) 055021, [1404.3716].

[44] J. Fan, S. M. Koushiappas and G. Landsberg, *Pseudoscalar Portal Dark Matter and New Signatures of Vector-like Fermions*, *JHEP* **01** (2016) 111, [1507.06993].

[45] A. Cuoco, B. Eiteneuer, J. Heisig and M. Krmer, *A global fit of the γ-ray galactic center excess within the scalar singlet Higgs portal model*, *JCAP* **1606** (2016) 050, [1603.08228].

[46] F. S. Sage and R. Dick, *Gamma ray signals of the annihilation of Higgs-portal singlet dark matter*, 1604.04589.

[47] A. Berlin, D. Hooper and G. Krnjaic, *Thermal Dark Matter From A Highly Decoupled Sector*, 1609.02555.

[48] A. Berlin, D. Hooper and G. Krnjaic, *PeV-Scale Dark Matter as a Thermal Relic of a Decoupled Sector*, *Phys. Lett.* **B760** (2016) 106–111, [1602.08490].

[49] D. Hooper, *Is the CMB telling us that dark matter is weaker than weakly interacting?*, *Phys. Rev.* **D88** (2013) 083519, [1307.0826].

[50] N. Fornengo, A. Riotto and S. Scopel, *Supersymmetric dark matter and the reheating temperature of the universe*, *Phys. Rev.* **D67** (2003) 023514, [hep-ph/0208072].

[51] G. Gelmini, P. Gondolo, A. Soldatenko and C. E. Yaguna, *The Effect of a late decaying scalar on the neutralino relic density*, *Phys. Rev.* **D74** (2006) 083514, [hep-ph/0605016].

[52] G. Kane, K. Sinha and S. Watson, *Cosmological Moduli and the Post-Inflationary Universe: A Critical Review*, *Int. J. Mod. Phys.* **D24** (2015) 1530022, [1502.07746].

[53] A. V. Patwardhan, G. M. Fuller, C. T. Kishimoto and A. Kusenko, *Diluted equilibrium sterile neutrino dark matter*, *Phys. Rev.* **D92** (2015) 103509, [1507.01977].

[54] H. Davoudiasl, D. Hooper and S. D. McDermott, *Inflatable Dark Matter*, *Phys. Rev. Lett.* **116** (2016) 031303, [1507.08660].

[55] D. H. Lyth and E. D. Stewart, *Thermal inflation and the moduli problem*, *Phys. Rev.* **D53** (1996) 1784–1798, [hep-ph/9510204].

[56] T. Cohen, D. E. Morrissey and A. Pierce, *Changes in Dark Matter Properties After Freeze-Out*, *Phys. Rev.* **D78** (2008) 111701, [0808.3994].

[57] T. Boeckel and J. Schaffner-Bielich, *Little inflation at the cosmological QCD phase transition*, Phys. Rev. D **85** (May, 2012) 103506, [1105.0832].

[58] T. Boeckel and J. Schaffner-Bielich, *A Little Inflation in the Early Universe at the QCD Phase Transition*, *Physical Review Letters* **105** (July, 2010) 041301, [0906.4520].

[59] K. Griest and D. Seckel, *Three exceptions in the calculation of relic abundances*, *Phys. Rev.* **D43** (1991) 3191–3203.

[60] J. Edsjo and P. Gondolo, *Neutralino relic density including coannihilations*, *Phys. Rev.* **D56** (1997) 1879–1894, [hep-ph/9704361].

[61] D. Tucker-Smith and N. Weiner, *Inelastic dark matter*, *Phys. Rev.* **D64** (2001) 043502, [hep-ph/0101138].

[62] Y. Cui, D. E. Morrissey, D. Poland and L. Randall, *Candidates for Inelastic Dark Matter*, *JHEP* **05** (2009) 076, [0901.0557].